

1-15-2012

Optimization of Magnetic Powdered Activated Carbon for Aqueous Hg(II) Removal and Magnetic Recovery

Emily K. Faulconer

University of Florida, faulcone@erau.edu

Natalia Hoogesteijn von Reitzenstein

University of Florida

David W. Mazyck

University of Florida

Follow this and additional works at: <http://commons.erau.edu/db-physical-sciences>

 Part of the [Environmental Chemistry Commons](#), and the [Materials Chemistry Commons](#)

Scholarly Commons Citation

Faulconer, E. K., Hoogesteijn von Reitzenstein, N., & Mazyck, D. W. (2012). Optimization of Magnetic Powdered Activated Carbon for Aqueous Hg(II) Removal and Magnetic Recovery. *Journal of Hazardous Materials*, 199-200(). Retrieved from <http://commons.erau.edu/db-physical-sciences/48>

This Article is brought to you for free and open access by the College of Arts & Sciences at Scholarly Commons. It has been accepted for inclusion in Department of Physical Sciences - Daytona Beach by an authorized administrator of Scholarly Commons. For more information, please contact commons@erau.edu.

Optimization of Magnetic Powdered Activated Carbon for Aqueous Hg(II) Removal and Magnetic Recovery

*Emily K. Faulconer^{*a}, Natalia V. Hoogesteijn von Reitzenstein^a, David W. Mazyck^a*

^a Department of Environmental Engineering Sciences, University of Florida, 217 Black Hall,
P.O. Box 116450, Gainesville, FL, 32611-645, (phone) 1.434.485.9021, (fax) 1.352.392.3076
emily.faulconer@yahoo.com

* Corresponding author. Tel/Fax: 434 485 9021, 352 3923076. E-mail address: emily.faulconer@yahoo.com (E.K. Faulconer)

Abstract

Activated carbon is known to adsorb aqueous Hg(II). MPAC (magnetic powdered activated carbon) has the potential to remove aqueous Hg to less than 0.2 µg/L while being magnetically recoverable. Magnetic recapture allows simple sorbent separation from the waste stream while an isolated waste potentially allows for mercury recycling. MPAC Hg-removal performance is verified by mercury mass balance, calculated by quantifying adsorbed, volatilized, and residual aqueous mercury. The batch reactor contained a sealed mercury-carbon contact chamber with mixing and constant N₂(g) headspace flow to an oxidizing trap. Mercury adsorption was performed using spiked ultrapure water (100 µg/L Hg). Mercury concentrations were obtained using EPA method 245.1 and cold vapor atomic absorption spectroscopy. MPAC synthesis was optimized for Hg removal and sorbent recovery according to the variables: C:Fe, thermal oxidation temperature and time. The 3:1 C:Fe preserved most of the original sorbent surface area. As indicated by XRD patterns, thermal oxidation reduced the amorphous characteristic of the iron oxides but did not improve sorbent recovery and damaged porosity at higher oxidation temperatures. Therefore, the optimal synthesis variables, 3:1 C:Fe mass ratio without thermal oxidation, which can achieve 92.5% (± 8.3%) sorbent recovery and 96.3% (±9%) Hg removal. The mass balance has been closed to within approximately ±15%.

Keywords: activated carbon; magnetic sorbent; mercury adsorption

1. Introduction

Mercury (Hg), a toxin that has been shown to bioaccumulate, can enter the environment from anthropogenic sources such as chlor-alkali wastewater and has severe health effects on humans, animals, and the environment [1]. The treatment of mercury-contaminated water remains a challenge, particularly due to the very low regulatory concentrations. Due to its listing as a toxic

pollutant under section 307(a) of the Clean Water Act (CWA), site-specific technology-based aqueous Hg effluent limits are regulated through the National Pollutant Discharge Elimination System (NPDES) permitting system. Any discharge to impaired water must not exceed the Total Maximum Daily Load (TMDL), the maximum allowable amount of a pollutant that a particular body of water can receive and still meet water quality standards. States have the power to require lower effluent limits, as is the case in the Great Lakes region where the limit has been set to less than 1 µg/L. The EPA has determined the water quality criteria for the protection of wildlife and for the protection of human health to be 1.3 ng/L and 1.8 ng/L, respectively [2,3]. Adsorption can be used as a polishing technique to reach lower wastewater effluent concentrations [4].

Activated carbon is known to remove Hg(II) from aqueous solutions [5-10]. MPAC has the potential to lower wastewater effluent mercury concentrations from industries such as chlor-alkali and coal-fired power plants utilizing flue gas desulfurization to less than 0.2 µg/L (the analytical detection limit using cold vapor atomic absorption (CVAA) spectroscopy) while being magnetically recoverable from solution. Traditional filtration methods to separate dispersed activated carbon from aqueous solution are susceptible to filter blockages and head loss. Magnetic recapture allows for simple separation of the sorbent from the waste stream and increases the ease of residuals management according to the cradle to grave responsibility of the Resource Conservation and Recovery Act (RCRA).

Magnetic adsorbents are an attractive solution for metallic and organic aqueous pollutants, particularly due to the simple magnetic separation process. Magnetic iron oxides have been used to synthesize new adsorbents utilizing multiwalled carbon nanotubes for Pb, 1-naphthol, Ni, Sr, and Eu adsorption [11-13], zeolites for Cr, Cu, and Zn adsorption [14], activated carbon for phenol, chloroform, and chlorobenzene adsorption [15], and dimercaptosuccinic acid for Hg, Ag,

Pb, Cd, and Tl adsorption [16]. However, these adsorbents have been applied to only a limited number of contaminants and mercury has thus far been largely overlooked. The available literature does not discuss the ratio of sorbent to iron oxide for either optimal adsorption or optimal magnetic recovery. Additionally, the potential for increased magnetic recovery from thermal oxidation of the iron oxides has not been investigated.

In this study, the adsorption of Hg(II) onto MPAC was studied in a batch system with respect to the synthesis variables of C:Fe mass ratio and thermal oxidation temperature and duration. Thermal oxidation was performed on the synthesized MPACs with the purpose of converting amorphous iron oxides formed during synthesis to magnetic iron oxides such as magnetite or maghemite. The goal of this study was to identify the synthesis variables for both optimal aqueous Hg removal and optimal sorbent recovery.

2. Materials and Methods

2.1 Materials

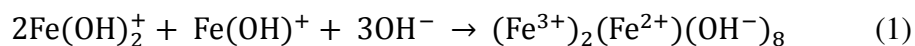
Solutions were prepared using ultrapure Type I water with a resistivity of 18.2 M Ω and a conductivity of 0.055 μ S. A commercially available bituminous coal-based powdered activated carbon (Calgon WPH) with a surface area of 1020 m²/g was oven-dried at 100°C for a minimum of 24 h prior to use. Hg(II) solutions were prepared by diluting 1000 mg/L stock Hg(NO₃)₂ (Fisher Scientific) in ultrapure water. The oxidizing purge trap to capture volatilized Hg was prepared using 4% w/v potassium permanganate (Fisher Scientific) in 10% sulfuric acid (Fisher Scientific) solution. The total digestion of MPAC was performed using 400 μ L aqua regia (3:1 v/v concentrated hydrochloric acid (J.T. Baker) to concentrated nitric acid (Fisher Scientific)), 2 mL of concentrated hydrofluoric acid (Acros Organics), and 20 mL of saturated boric acid solution (Acros Organics). According to EPA method 245.1, the heated digestion for Hg

quantification was performed using concentrated nitric acid (Fisher Scientific), concentrated sulfuric acid (Fisher Scientific), 5% w/v potassium permanganate (Fisher Scientific), 5% w/v potassium persulfate (Fisher Scientific), and 12% w/v sodium chloride – hydroxylamine sulfate solution (Fisher Scientific).

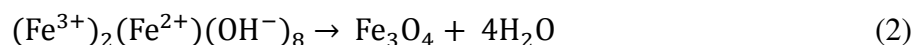
2.2 MPAC Synthesis

MPAC composites were synthesized at room temperature by heterogeneous nucleation [17]. Fe(II) and Fe(III) salts (ferric chloride (FeCl_3) and ferrous-ferric oxide (FeO , Fe_2O_3)) were dissolved in ultrapure water with mechanical stirring. After carbon addition, rapid alkaline hydrolysis was induced by adding 5M NaOH drop wise to the solution to reach pH 10. The hydrolysis products, $\text{Fe}(\text{OH})^+$ and $\text{Fe}(\text{OH})_2^+$, reacted to form ferrihydrite which preferentially precipitated onto the carbon surface but, due to thermodynamic instability, transformed into magnetite (Fe_3O_4) (Eq. 1 and 2 [18]). In the presence of atmospheric oxygen, the magnetite is susceptible to oxidation to maghemite [19].

Generation of ferrihydrite intermediate:



Dehydration of ferrihydrite, formation of magnetite:



The amount of activated carbon was adjusted to obtain 1:1, 2:1, and 3:1 C:Fe mass ratios. Samples were rinsed with ultrapure water to remove residual NaOH until a constant water contact pH was achieved and subsequently oven-dried at 100°C overnight.

Although maghemite is likely the predominant iron species present on the MPAC surface due to the synthesis technique used, small amounts of non-magnetic iron oxides (e.g. hematite, amorphous iron oxides) may occur. Thermal oxidation may convert some of these amorphous

iron oxides to magnetic iron oxides such as magnetite or maghemite [19]. To compare the initial synthesis product to one having undergone thermal oxidation, representative portions of the original MPAC were subjected to oxidation in a box furnace with air flow with varying temperatures (250°C, 350°C, and 450°C) and durations (0, 3, and 6 h).

2.3 MPAC Characterization

The surface area was measured by a surface area analyzer (Quantachrome Instruments NOVA 2200e). Each sample was outgassed at 110°C for 24 hours before being placed in a 77K liquid nitrogen bath with nitrogen gas adsorbate. The surface area of each sample was calculated by the Brunauer-Emmett-Teller (BET) equation [20]. Using the adsorption isotherm, the pore size distributions over the mesopore region were calculated using the Barrett-Joyner-Halenda (BJH) equation [21].

The X-ray diffraction (XRD) patterns of the MPAC were recorded using a Philips APD 3720 X-ray unit. XRD patterns were analyzed to identify the iron speciation on the MPAC surface. Compounds were identified using the powder diffraction identification number according to the International Centre for Diffraction Data.

The MPAC, easily dispersed in aqueous solution, can be retrieved using a strong magnet such as neodymium, a rare-earth magnet. The recovery (%) of MPAC from aqueous solution and sorbent mass balance was determined using the dry mass captured by the magnet, the dry mass retained by a 0.45µm nitrocellulose filter after vacuum filtration, and the mass of the initial MPAC dose. The contact time (5 min) and carbon dose (1 g/L) were held constant while the MPAC species varied based on synthesis variables. Preliminary experimentation indicated the use of a 5 min contact time because the results were not significantly different than a 10 or 30 min contact time while a 1 min contact time produced considerably lower magnetic sorbent

recovery from aqueous solution. Iron effluent levels were quantified using a spectrophotometer (Hach DR/4000 Spectrophotometer and TPTZ powder pillow method 2190).

2.4 Adsorption Experiments

In order to ensure future experiments were performed at adsorption equilibrium, the contact time required to reach Hg adsorption equilibrium onto MPAC was investigated. A 1 g/L dose of MPAC was applied to 100 µg/L Hg solution for 0 - 180 minutes.

MPAC Hg-removal performance was verified by integral mass balance of Hg. Based on published aqueous Hg(II) mass balances, acceptable mass balance closure was determined to be within approximately $\pm 15\%$ [22,23]). This was achieved by quantifying the residual aqueous Hg, adsorbed Hg extracted from MPAC by HF digestion, and volatilized Hg captured in the KMnO₄ trap. Trace levels of Hg, 0.125 µg Hg / g virgin activated carbon, were determined via aqua regia and hydrofluoric acid digestion and these values considered in the mass balance. The MPAC dose (1 g/L), Hg concentration (100 µg/L), and contact time (180 min) were held constant.

The batch reactor contained a sealed Teflon mercury-carbon contact chamber with 0.8 L/min headspace N₂ flow through an inlet/outlet port to an oxidizing purge trap. The MPAC was applied at a 1g/L dose to 100 µg/L Hg-spiked ultrapure water (Hg(NO₃)) and magnetically mixed for 180 min contact time at room temperature. After the specified contact time, the adsorbent was separated via filtration using 0.45µm nitrocellulose filter and the reactor rinsed with 20% (v/v) HNO₃ in ultrapure water. Metal concentrations were measured using EPA digestion method 245.1 and cold vapor atomic adsorption spectroscopy (CVAA).

2.5 Data Analysis

All experiments were performed in triplicate and average values reported. All replicate data falls within the 95% confidence interval. Error bars represent the standard error of the mean. The Box

Behnken experimental design for response surface methodology was used to identify the optimal MPAC for Hg removal according to the three variables specified. The design required 17 total runs with 12 experiments and 5 replicates of the center point. The experimental design was analyzed using Design-Expert software (version 6.0.5).

3. Results and Discussion

3.1 Adsorbent Characterization: Porosity

The process of iron impregnation onto the carbon was expected to reduce the available surface area relative to the virgin activated carbon due to the minimal surface area of the iron oxides (1.9 m²/g). As expected, the 1:1 C:Fe resulted in approximately a 50% reduction of surface area from 1020 m²/g to 551 m²/g while the 2:1 and 3:1 C:Fe showed surface areas reduced by the expected ~33% and 25% to 709 m²/g and 790 m²/g, respectively. As predicted, the available surface area increased as the loading ratio (C:Fe) increased (Table 1). The surface areas reported have a relative standard deviation (RSD) of approximately 7%.

Portions of the synthesized MPAC were subjected to thermal oxidation for varying temperatures and durations (250°C, 350°C, and 450°C for 0, 3, and 6 hours). Figure 1a-c demonstrates that oxidation of a 1:1 C:Fe MPAC at 250°C had little effect on the porosity regardless of duration. Thermal oxidation at 350°C and 450°C reduced the surface area and pore volume while increasing the pore size. The surface area loss and degradation of pores are likely due to decomposition of surface oxygen groups and gasification of carbon at temperatures over approximately 400°C [7]). Although surface area can influence adsorption capabilities, it may not be directly related to the efficiency of Hg(II) removal; adsorption efficiency can be influenced by other sorbent characteristics such as surface oxygen functionality [8,24]). This

study shows a poor correlation of 0.472 for surface area and mercury removal (calculated using Design-Expert software).

The unoxidized 1:1, 2:1, and 3:1 C:Fe MPACs exhibited similar partial BJH pore size distributions (PSD) to the virgin PAC (Fig 2) as calculated from nitrogen adsorption isotherms. The furnace oxidation of the samples caused pore degradation/collapse, demonstrated by the reduction in cumulative pore volume and slight skewing of the pore volume to higher pore diameters, seen in the highly oxidized sample (450°C, 6h). PSD replicates indicated no greater than a 5.5% RSD.

3.2 Adsorbent Characterization: XRD

Although maghemite is the most likely iron oxide produced in the synthesis of MPAC, other iron oxides have the potential to precipitate onto the carbon surface. XRD data (not presented here) indicated no significant difference in iron speciation between the 1:1, 2:1 and 3:1 C:Fe MPAC samples. XRD analysis was performed to identify the iron oxides present on un-oxidized 3:1 C:Fe as well as 3:1 C:Fe samples subjected to oxidation for 6 hours at 250°C, 350°C, and 450°C, respectively (Figure 3).

All oxidation temperatures investigated displayed peaks with positions and relative intensities that match well with those for maghemite-c (39-1346) and maghemite-q (25-1402). At over 400°C, additional peaks were identified as hematite (33-0664), a non-magnetic iron oxide. All major diffraction peaks were associated with the iron oxides identified. Increased oxidation temperature, particularly 450°C, reduced the amorphous characteristic of the iron oxides on the MPAC, seen in the progressively flattened baseline with increased furnace temperature.

3.3 Adsorbent Recovery

MPAC was retrieved from aqueous solution via magnetic solid-phase extraction. The sorbent recovery was not significantly influenced by the C:Fe, oxidation temperature or duration with all MPACs investigated reaching a sorbent recovery rate ranging from 75 -91% (RSD 7%).

3.4 Effect of Contact Time

A 1 g/L dose of MPAC was applied to 100 µg/L Hg solution to study the effect of contact time on the adsorption of Hg(II) shown in Figure 4. The initial adsorption rate was rapid with over 90% of the Hg(II) removed during the first minute of contact. This was followed by a much slower adsorption rate, reaching pseudo-equilibrium at 120 min. Before carbon addition, the solution is approximately pH 4.5 with a percentage change in the pH of 6.5% in the first 30 seconds of contact but stabilizing to a percentage change in pH of 27-34% for contact times 5 minutes through 180 minutes.

Typically, iron is not a concern from a regulatory standpoint and is commonly a constituent of industrial wastewaters. The adsorbent is quite stable and Fe effluent concentrations fell below the detection limit (0.022mg/L total Fe) for all contact times, 0.5 – 180 minutes.

3.5 Hg Mass Balance

Prior to performing the Hg adsorption experiments, it was imperative to perform control runs. An air blank, performed on the test stand with only ultrapure water in the mercury-carbon contact chamber, verified that the batch reactor was free from residual Hg contamination. A sorbent blank identified trace levels of Hg present in the MPAC (0.125 ± 0.055 µg Hg / g MPAC).

MPAC is synthesized using a coal-based activated carbon; coal is known to contain trace levels of Hg. This background level of Hg was taken into account for the mass balance calculations. A background analysis was performed by running Hg-spiked ultrapure water through the batch reactor in the absence of carbon. The analysis, presented in Figure 5a, revealed the following:

low levels of Hg volatilization occurred in the absence of carbon, quantifiable Hg residues (approximately 9% total Hg) formed in test stand labware necessitating a HNO₃ rinse to fully quantify the residual Hg, and 6% Hg was fugitive. The fugitive Hg was likely due to mass and volume measurement errors amplified by the small scale of the experiment.

The mass balance for Hg adsorption onto 3:1 C:Fe MPAC is presented in Figure 5b. At unadjusted pH, approximately 91% of the Hg was removed from aqueous solution with 2% volatilized and 84% adsorbed while 4% remained fugitive. The average mass balance closure for all 17 experiments was 99.5% with a standard deviation of 8.8%. The mass balance closures ranged from 88.3% to 116.8% but many runs did not fall within the 95% confidence intervals; the observed distribution fits a random distribution curve. The challenge in obtaining mass balance closure was likely due to HF extraction inefficiency in quantifying the adsorbed Hg, mechanical loss of C resulting in lower Hg masses extracted in the HF digestion, and volumetric measurement errors amplified due to the small scale of the experiment.

Aqueous pH greatly influences Hg(II) speciation as well as activated carbon surface chemistry, therefore influencing removal. At a pH below the point of zero charge (pH_{PZC}) cationic mercury species (e.g. Hg²⁺, HgOH⁺, and HgCl⁺) must overcome electrostatic repulsion by the protonated surface oxygen groups in order to undergo ion exchange while anionic species (HgCl₃⁻, HgCl₄²⁻) are attracted to the positive carbon surface. At pH values above the sorbent pH_{PZC}, cationic Hg species are electrostatically attracted to the surface while anions are repelled by the negative sorbent surface. Uncharged Hg species such as Hg(OH)₂ and HgCl₂ are removed by physisorption. Hg(OH)₂ has the potential to precipitate from solution. The unadjusted matrix pH is ~4.5. Using the speciation program Visual MINTEQ 2.61, the mercury speciation in the given matrix conditions was determined to be HgOH⁺ and Hg(OH)₂. The Hg(OH)₂ likely

preferentially precipitated on the MPAC surface once maximum solubility was reached. The HgOH^+ was likely removed via physisorption and ion exchange. Future work will investigate the influence of matrix pH and pCl on the mercury speciation and binding mechanisms.

3.6 Optimization

Figure 6 demonstrates that the thermal oxidation temperatures investigated in this study do not influence the aqueous mercury removal capabilities of MPAC despite the pore damage incurred at oxidation temperatures over 250°C. At all oxidation temperatures, the 3:1 MPAC achieved the highest mercury removal. The 1:1 and 2:1 C:Fe performed similarly for Hg removal, with coefficient of variation (CV) values under 6% at each temperature. In addition to oxidation temperature, the MPAC Hg removal performance was unaffected by thermal oxidation time at all temperatures investigated; with CV values ranging from 2%-6.5%.

Box Behnken fractional factorial design was used to identify the optimal MPAC for both Hg removal and MPAC recovery (equally weighted in the experimental design) according to the following variables: C:Fe, and thermal oxidation temperature and time. The following criteria were used in the numerical optimization: C:Fe within range, minimized oxidation temperature and time, maximized magnetic recovery, and maximized Hg removal. Oxidation parameters were minimized to reduce the cost of MPAC synthesis. Based on these criteria, the optimal synthesis variables of 3:1 C:Fe with no furnace oxidation would achieve a predicted sorbent recovery of 92.5% ($\pm 8.3\%$) and Hg removal of 96.3% ($\pm 9\%$).

3.7. Conclusions

The original powdered activated carbon was modified by iron impregnation and thermal oxidation to allow for magnetic recovery of the sorbent. The MPAC synthesis was optimized for mercury removal and magnetic recovery according to the carbon to iron ratio and thermal

oxidation temperature and duration. The process of iron impregnation reduced the surface area as expected, with the 3:1 C:Fe effectively allowing for significant magnetic sorbent recovery while preserving most of the original sorbent surface area. Thermal oxidation decreased the amorphous characteristic of the MPACs but did not provide a significant increase in magnetic recovery or Hg-removal performance. The potential benefits of decreased amorphous characteristic are not realized and also outweighed by the damaged porosity and increased cost in production.

When the 3:1 C:Fe MPAC was applied to 100 µg/L Hg solution with unadjusted pH, approximately 91% of the Hg was removed from aqueous solution with 2% volatilized, 84% adsorbed, and 4% remained fugitive. The achieved mercury removal of the unoxidized 3:1 C:Fe MPAC aligns well with the predicted optimal sorbent determined by using the Box Behnken fractional factorial approach. The average mass balance closure for all 17 runs was 99.5% with a standard deviation of 8.8%, verifying the MPAC Hg removal performance.

An objective of this study was to produce an activated carbon that was capable of being magnetically separated from the aqueous phase while retaining the high adsorption capacity of the virgin activated carbon. Various carbon to iron ratios and thermal oxidation temperatures were investigated and analyzed based on surface area, magnetic recovery, and mercury removal performance in order to identify the optimal synthesis variables. A 3:1 C:Fe without thermal oxidation produces a composite that can easily be recovered magnetically while preserving surface area and maximizing mercury adsorption.

Acknowledgments

We thank Valenciu Craciun, Ph.D. and the Major Analytical Instrumentation Center (MAIC) at the University of Florida for support. We express particular appreciation to Katrina Indarawis, Carmen Ceron and Kelsie Timpe for their assistance.

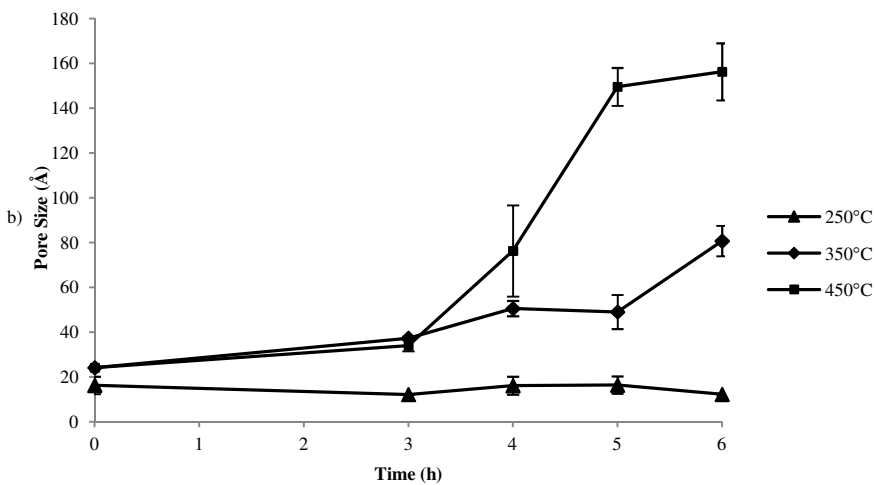
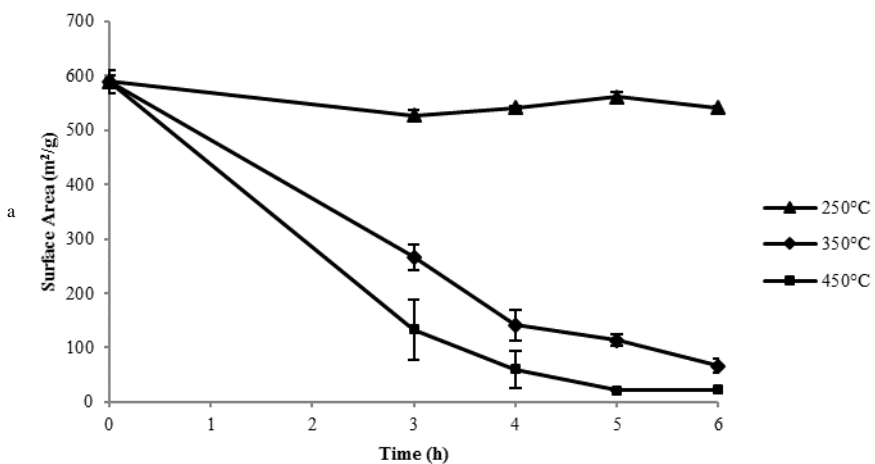
References

- (1) U.S. Environmental Protection Agency. Mercury study report to congress, volume II: An inventory of anthropogenic mercury emissions in the United States. 1997.
- (2) Code of Federal Regulations. Water Quality Criteria for the Protection of Wildlife. 2010;40CFR132 Table 4.
- (3) Code of Federal Regulations. Water Quality Criteria for Protection of Human Health. 2010;40CFR132 Table 3.
- (4) US Environmental Protection Agency, Office of Superfund Remediation and Technology Innovation. Treatment technologies for mercury removal from soil, waste, and water. 2007.
- (5) Huang CP, Blankenship DW. The Removal of Mercury(II) from Dilute Aqueous-Solution by Activated Carbon. *Water Res.* 1984;18(1):37-46.
- (6) Humenick MJ, Schnoor JL. Improving Mercury (II) Removal by Activated Carbon. *Journal of the Environmental Engineering Division-Asce* 1974;100(NEE6):1249-1262.
- (7) Bansal R, Goyal M. Activated carbon adsorption. Boca Raton: CRC Press; 2005.
- (8) Marsh H, Rodriguez-Reinoso F. Activated Carbon. Amsterdam: Elsevier; 2006.
- (9) Lopez-Gonzalez J, Moreno-Castilla C, Guerrero-Ruiz A, Rodriguez-Reinoso F. Effect of Carbon-Oxygen and Carbon-Sulphur Surface Complexed on the Adsorption of Mercuric Chloride in Aqueous Solutions by Activated Carbons. *J. Chem. Tech. Biotechnol.* 1982;32:575-579.
- (10) Krishnan KA, Anirudhan TS. Removal of mercury(II) from aqueous solutions and chlor-alkali industry effluent by steam activated and sulphurised activated carbons prepared from bagasse pith: kinetics and equilibrium studies. *J.Hazard.Mater.* 2002 MAY 27;92(2):161-183.
- (11) Hu J, Shao D, Chen C, Sheng G, Li J, Wang X, et al. Plasma-Induced Grafting of Cyclodextrin onto Multiwall Carbon Nanotube/Iron Oxides for Adsorbent Application. *J Phys Chem B* 2010 MAY 27;114(20):6779-6785.

- (12) Chen C, Hu J, Shao D, Li J, Wang X. Adsorption behavior of multiwall carbon nanotube/iron oxide magnetic composites for Ni(II) and Sr(II). *J.Hazard.Mater.* 2009 MAY 30;164(2-3):923-928.
- (13) Chen CL, Wang XK, Nagatsu M. Europium Adsorption on Multiwall Carbon Nanotube/Iron Oxide Magnetic Composite in the Presence of Polyacrylic Acid. *Environ.Sci.Technol.* 2009 APR 1;43(7):2362-2367.
- (14) Oliveira LCA, Petkowicz DI, Smaniotto A, Pergher SBC. Magnetic zeolites: a new adsorbent for removal of metallic contaminants from water. *Water Res.* 2004 OCT;38(17):3699-3704.
- (15) Oliveira LCA, Rios RVRA, Fabris JD, Garg V, Sapag K, Lago RM. Activated carbon/iron oxide magnetic composites for the adsorption of contaminants in water. *Carbon* 2002;40(12):2177-2183.
- (16) Yantasee W, Warner CL, Sangvanich T, Addleman RS, Carter TG, Wiacek RJ, et al. Removal of heavy metals from aqueous systems with thiol functionalized superparamagnetic nanoparticles. *Environ.Sci.Technol.* 2007 JUL 15;41(14):5114-5119.
- (17) Schwertmann U, Cornell RM. Iron oxides in the laboratory : preparation and characterization. 2 completely rev a exte ed. Weinheim ; New York: Wiley-VCH; 2000.
- (18) Perez OP, Umetsu Y, Sasaki H. Precipitation and densification of magnetic iron compounds from aqueous solutions at room temperature. *Hydrometallurgy* 1998 NOV;50(3):223-242.
- (19) Cornell R, Schwertmann U. The Iron Oxides. Weinheim: VCH; 1996.
- (20) Brunauer S, Emmett PH, Teller E. Adsorption of gases in multimolecular layers. *J.Am.Chem.Soc.* 1938 JAN-JUN;60:309-319.
- (21) Barrett EP, Joyner LG, Halenda PP. The Determination of Pore Volume and Area Distributions in Porous Substances .1. Computations from Nitrogen Isotherms. *J.Am.Chem.Soc.* 1951;73(1):373-380.
- (22) Looney BB, Denham ME, Vangelas KM, Bloom NS. Removal of mercury from low-concentration aqueous streams using chemical reduction and air stripping. *Journal of Environmental Engineering-Asce* 2003 SEP;129(9):819-825.
- (23) Balogh SJ, Nollet YH. Mercury mass balance at a wastewater treatment plant employing sludge incineration with offgas mercury control. *Sci.Total Environ.* 2008 JAN 15;389(1):125-131.
- (24) Carrott PJM, Carrott MMLR, Nabais JMV. Influence of surface ionization on the adsorption of aqueous mercury chlorocomplexes by activated carbons. *Carbon* 1998;36(1-2):11-17.

Table 1.

C:Fe	Furnace Temp. [°C]	Time (h)	Surface Area	pHPZC
1:1	350	0	551.23	9.23
2:1	450	0	709.04	9.39
3:1	350	0	790.11	9.51
3:1	450	3	46.86	6.55



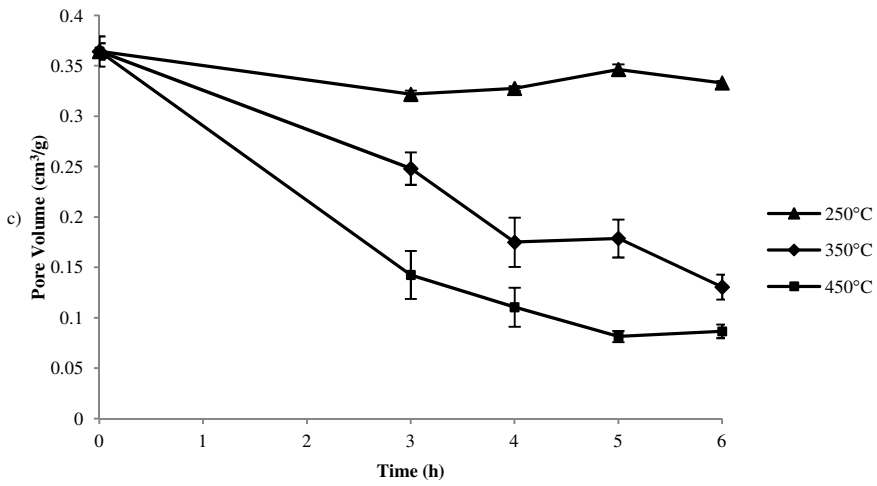


Figure 1.

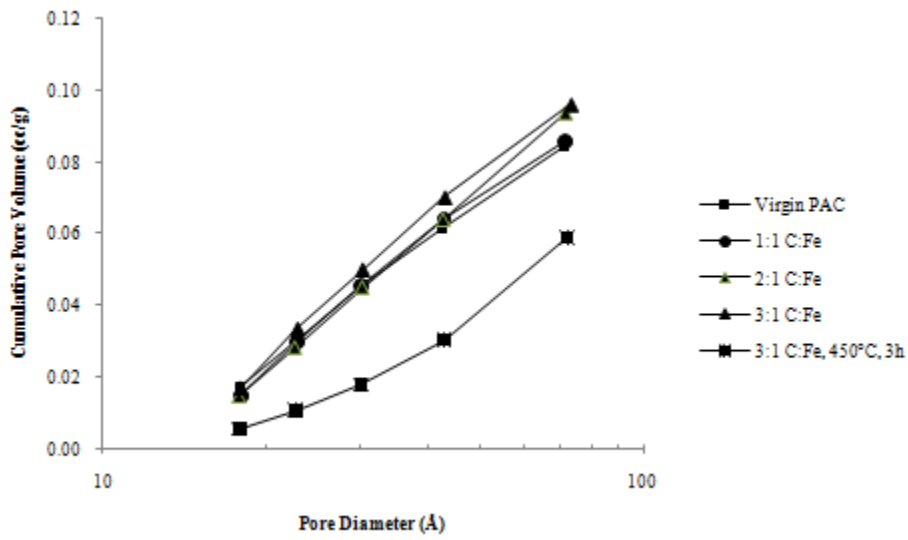


Figure 2.

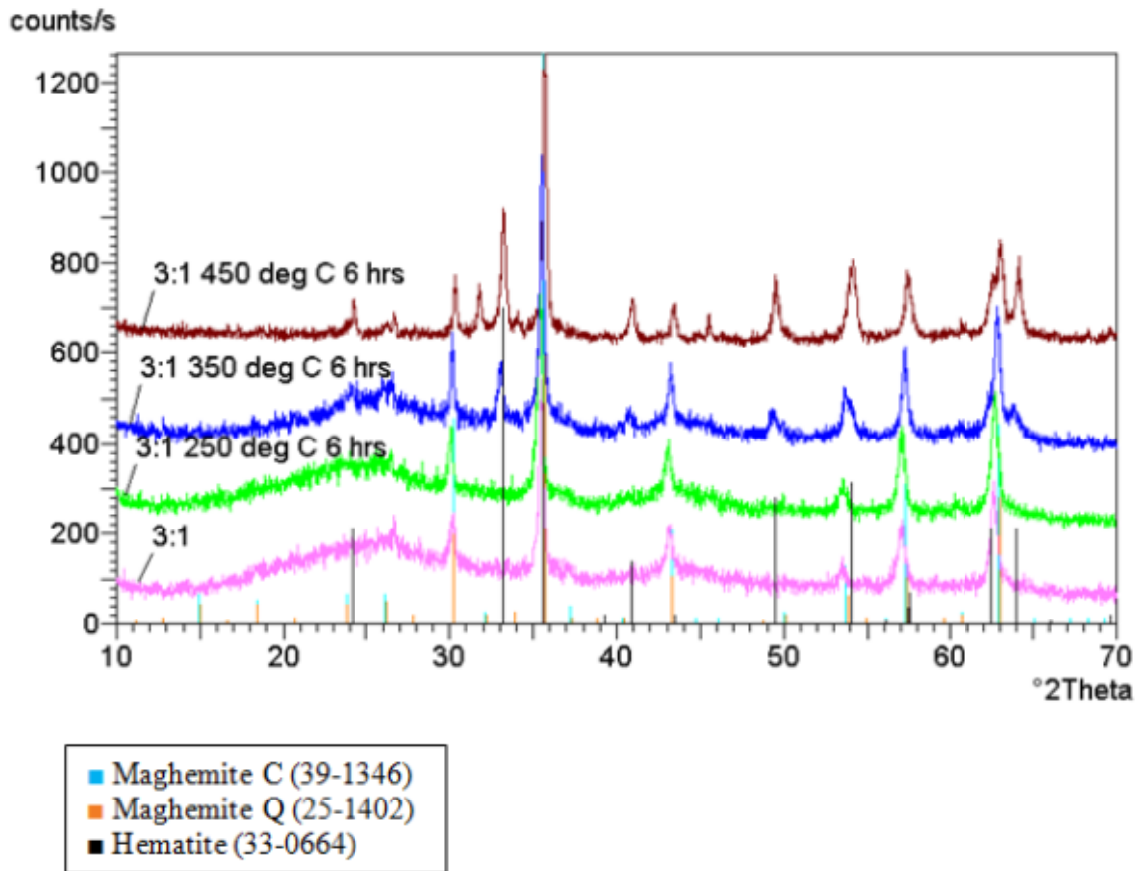


Figure 3.

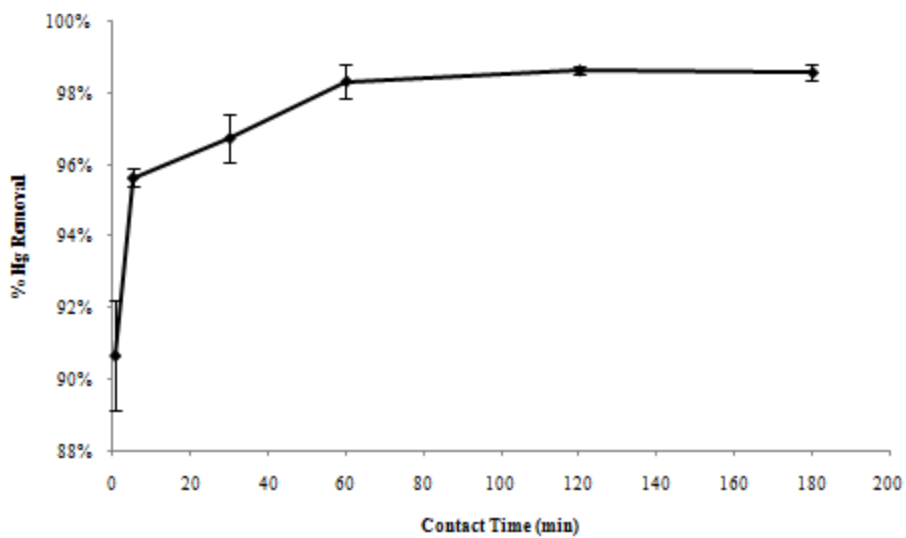


Figure 4.

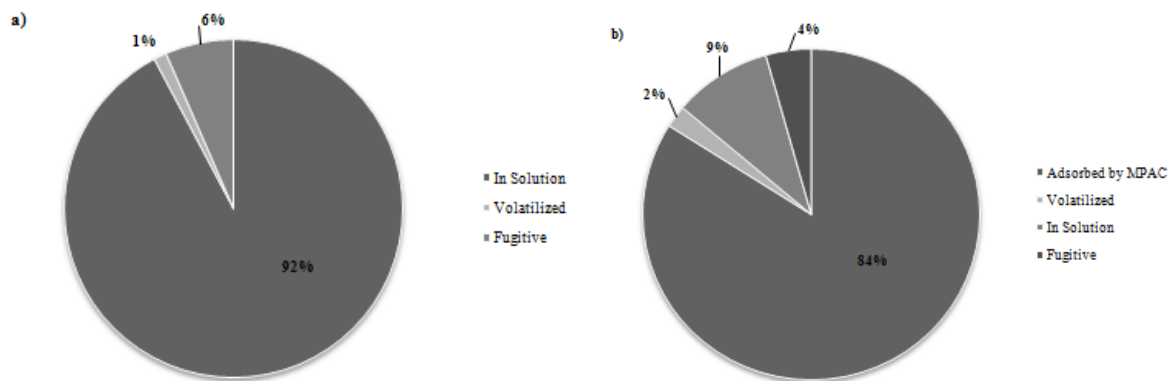


Figure 5.

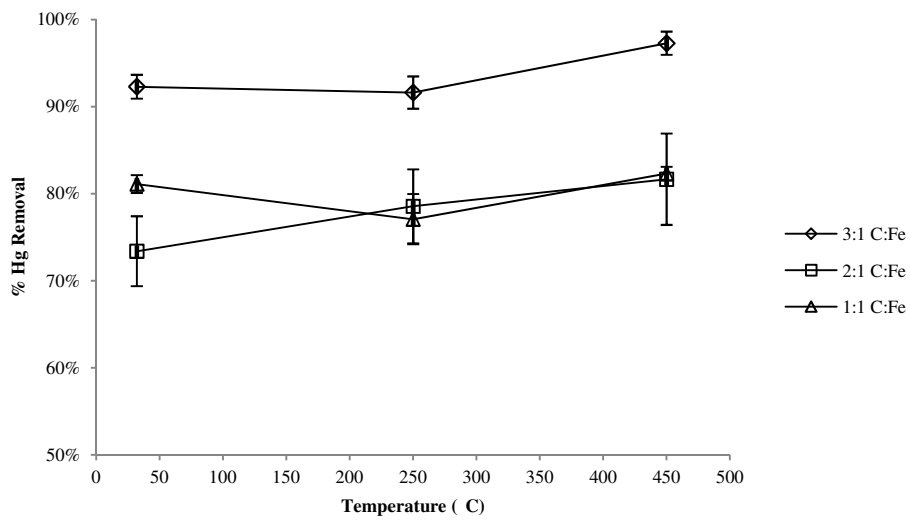


Figure 6.